Acta Oceanol. Sin., 2017, Vol. 36, No. 5, P. 31–43
DOI: 10.1007/s13131-017-1054-7
http://www.hyxb.org.cn
E-mail: hyxbe@263.net

Experimental analysis of infragravity waves in two eroded microtidal beaches

MARIO Conde-Frias[1]*, LUIS Otero[1], JUAN Camilo Restrepo[1], JUAN Carlos Ortíz[1]

[1] Geosciences Research Group GEO4, Department of Physics, Universidad del Norte, Barranquilla 081007, Colombia

Received 8 August 2016; accepted 29 September 2016

Abstract

This work aims to contribute to the characterization and understanding of infragravity waves on two beaches with erosion problems. For this reason, we have used an array of ADCP and a pressure sensor to measure wave parameters and pressure inside and outside of the surf zone during the dry and rainy period in the beaches of Galerazamba and Manzanillo del Mar (both dissipative and eroded beaches) located in the Colombian Caribbean coast. Based on these measurements, we have carried out a spectral analysis in order to identify the frequency components that characterize the wave and its energy; thus, we identified the characteristic frequencies of infragravity waves to finally filter the infragravity signal on each beach in different seasonal periods. Among the results of the Welch spectrum applied to surface elevation time series, we found that, the frequencies' energy of the sea-swell band decreases due to bottom friction and wave breaking as the wave approaches the shore, while the frequencies' energy of the infragravity band increases significantly. In addition, for the wavelet analysis, we could observe how the energy of the infragravity band, especially the lowest frequencies gain energy as the waves approaches the coast. Furthermore, based on the infragravity wave obtained from the extreme wave event registered during the field campaign we can conclude that the contribution of this signal is important in the erosion problems presented in the beaches of Galerazamba and Manzanillo del Mar. Finally, these results show the need to realize other studies that allow us to understand deeply, the role of infragravity waves on the morphological changes that occurs in these beaches.

Key words: infragravity waves, long waves, experimental analysis, fourier analysis, wavelet transform

Citation: Mario Conde-Frias, Luis Otero, Juan Camilo Restrepo, Juan Carlos Ortíz. 2017. Experimental analysis of infragravity waves in two eroded microtidal beaches. Acta Oceanologica Sinica, 36(5): 31–43, doi: 10.1007/s13131-017-1054-7

1 Introduction

Describe complex phenomena such as sediment transport, coastal hydrodynamics modeling requires an accurate representation of the most complex interactions between small and large scale movements throughout the water column. Field and laboratory measurements shows that low frequency oscillations have an important contribution to the amount of energy within the surf zone (Aagaard and Bryan, 2003; Elgar et al., 1992).

In its generation zone, wave is generally comprised of waves with different directions and frequencies. These waves are classified and named according to their period as: gravity waves, those with periods between 1 s and 30 s; and infragravity waves, those with periods between 30 s and 300 s (Munk, 1949). There have been many breakthroughs in the field of short-period oscillations, which have made it possible to determine wave's parameters with high accuracy (e.g., Eckart, 1952; Elgar and Guza, 1985). However, despite the extensive theoretical work and laboratory and field experiments carried out in order to identify possible sources of infragravity energy, the exact mechanism of generation of these oscillations remains to be ascertained (Ruessink, 1998b).

Furthermore, adequate experimental information is not available, which prevents us from characterizing a forcing condition that reflects the interaction between short wave and long wave components, when applied to any of the developed theoretical models (Lara et al., 2004). Currently, it is known that this type of waves are oscillations of the mean sea level with periods ranging from 30–300 s (Munk, 1949); they are generated through two mechanisms, both associated with wave height modulation, in the wave groups scale. The first mechanism, through nonlinear interactions among incident short waves, is the releasing of the bound long waves when group structure of sea-swell waves is destroy in the breaking process (e.g., Dong et al. 2009a; Herbers et al., 1994; Longuet-Higgins and Stewart, 1962); In this approach, the short waves form a group structure that generate a second order wave of less frequency (called the bound long wave). The bound long wave travels with the group (means that the bound long wave celerity is the group celerity), when the short waves begin to break by the interaction with the beach slope, the group structure disappears and the bound long wave can propagate as a free long wave (with $c = \sqrt{gh}$). When the long wave is traveling with the group, its magnitude is in terms of centimeters, even decimeters in deep water (Webb et al., 1991); however, the magnitude of the long waves increase as these oscillations reach the coast by interaction with the beach slope (Lara et al., 2004). The second mechanism is through the varying breakpoint position (e.g., Dong et al. 2009b; Symonds et al., 1982), in this mechanism it is proposed that the point of break-

Foundation item: The Program of Administrative Department of Science, Technology and Innovation under contract No. COLCIENCIAS 03932013.
*Corresponding author, E-mail: mfrias@uninorte.edu.co

ing acts like a wave generator, where the long wave its generated by the interaction between the outgoing wave (produced by the changing of the breaking point) and the reflected one. It is important to highlight that the variation of breaking point do not assumed a bound wave, so the amplitude of the long wave depends on the phase difference between the incident and the reflected long wave.

Other studies (e.g., Guza and Thornton, 1982; Holman and Bowen, 1982; Holman and Sallenger, 1985) suggested that infragravity waves were related to coastal erosion, problems in coastal structures and coastal flooding (run-up) processes. Guza and Thornton (1982), Holman and Sallenger (1985), Oltman-Shay and Guza (1987), Wright et al. (1986) conducted the first field research on infragravity oscillations; however, since the breaking point, the wave energy and grouping factor cannot be controlled in these environments, it was difficult to study these waves on natural beaches. On the other hand, subsequent field studies showed that in some low-slope dissipative beaches (≈1:200), there was a reduced infragravity wave height rather than the expected increase (Ruessink, 1998a). Since these initial observations were made, many authors have reported several mechanisms of infragravity energy dissipation in recent literature. Henderson and Bowen (2002) suggested that bottom friction was the main mechanism of energy dissipation; however, because drag coefficient values for sandy beaches was too high in the bottom friction formulations, Henderson et al. (2006) suggested a nonlinear energy transfer from infragravity frequencies to sea and swell frequencies. On the other hand, laboratory measurements introduced the concept breaking of infragravity waves (e.g., Battjes et al., 2004; Van Dongeren et al., 2007; Lin and Hwung, 2012). Finally, De Bakker et al. (2014) showed that dissipation of infragravity wave depended on their frequencies. Infragravity waves with frequencies higher than ≈0.016 7 to 0.024 5 Hz dissipated as they reached the coast, while lower frequencies showed little energy dissipation.

In this study, we analyzed infragravity oscillations in microtidal beaches with erosion problems for two wave conditions (average and extreme condition), obtained from hydrodynamic measurements realized on dissipative beaches located on the Colombian Caribbean coast during two periods (dry and wet periods) (Fig. 1). We will specifically check energy changes in the infragravity band during average and extreme conditions to see the importance of this oscillation in these beaches, keeping in mind that previous studies associated the erosion problems of these beaches only to the gravity waves. Finally, we realized the spectral analysis (Fourier and wavelet analysis) in order to filter the signal and study the changes in wave height and dominant frequencies as the infragravity wave approaches the coast.

2 Materials and methods

2.1 *Study area*

To carry out the analysis of infragravity waves, we selected two beaches: Galerazamba and Manzanillo del Mar; located northwest of the Colombian Caribbean coast (Fig. 1).

Manzanillo del Mar and Galerazamba are dissipative beaches with slopes β_M=0.007 and β_G=0.001, respectively (Fig. 1). Thus in these beaches, especially in the surf zone and swash zone, the energy of the infragravity waves is higher than the energy of the gravity waves (Wright and Short, 1984). Due to their location in the Colombian Caribbean coast, they have a microtidal system (e.g., Restrepo et al., 2012). Wave climate for the continental shelf of both beaches is dominated by waves coming from the northeast and east-northeast. Nevertheless, this area is also affected by waves coming from the west and southwest to a lesser extent. At seasonal scale, wave variability depends on the seasonal period. There are two seasonal periods in Colombia as a result the Intertropical Convergence Zone (ITCZ) movement. The dry period runs from December to April. It is characterized by strong winds coming from the northeast, therefore, the largest waves are generated at this time of year (mean H_s=2.3 m). The rainy period runs from August to November. It is characterized by high rainfall and a decrease in wind speeds, resulting in a gentle swell (mean H_s=1.1 m) (Ortiz et al., 2013).

According to Rangel-Buitrago et al. (2015), the beaches of Galerazamba and Manzanillo del Mar present high erosion rates. The study showed that the coast line retreat on these beaches reaches up 1.5 m/a due to several causes as sea level rise and the strong waves of the zone associated with extreme events.

2.2 *Methodology*

To investigate the importance of infragravity waves in the beaches of Galerazamba and Manzanillo del Mar, it is necessary to obtain the infragravity wave component, to do that in both beaches were realized measurements of wave parameters like significant wave height (H_s), peak period, mean wave direction, currents and sea level in the surf zone during the dry and rainy period. We placed an ADCP and a pressure sensor in April (dry period) and November (rainy period) to observe the evolution of the infragravity wave in each of these beaches (Fig. 2).

The ADCP was moored 10 m deep to measure the wave every hour, with a burst length of 2 048 samples at a rate of 2 Hz. The pressure sensor was placed 1.9 m in the surf zone to carry out measurements every hour with a burst length of 2 048 samples at a rate of 2 Hz.

From the significant wave height time series measured by the ADCP during the dry and wet periods, an average condition and an extreme condition were defined for each beach, the average conditions refers to the mean condition presented in each period and the extreme condition is the highest value recorded by the ADCP in each beach in any period. The average condition for Manzanillo del Mar in the dry and wet period were 0.6 m and 0.5 m respectively, and the extreme condition was 0.86 m during the dry period. On the other hand, for Galerazamba the average condition in the dry and wet period were 1.2 m and 0.6 m, respectively and the extreme condition was 1.61 m during the dry period. The sea state chosen for graph the spectra of the mean (average) condition and extreme condition was obtain by selecting an specific date with the same values of significant wave height found in the average condition and in the extreme condition.

With the average and extreme condition already defined for each beach, we carried out an spectral analysis to the surface elevation time series associated to these conditions, in order to identify the frequency components that characterize the wave and its energy. The spectral analysis was carried out using a Welch periodogram, each section was windowed with a Hamming window, the total segments used was 8 with a 50% of overlapping.

Finally, we used the continuous wavelet transform (CWT) (Dong et al., 2008; Huang, 2004; Liu, 1994; Massel, 2001; Morlet et al., 1982) to characterize the propagation of the infragravity wave from the ADCP to the pressure sensor, around the dominant frequencies before and after reaching the surf zone. To achieve this, we followed the routine developed by Torrence and Compo (1998). The CWT (W_n) of a discrete sequence x_n is defined as the convolution of x_n with a scaled and translated version $\psi_0(\eta)$:

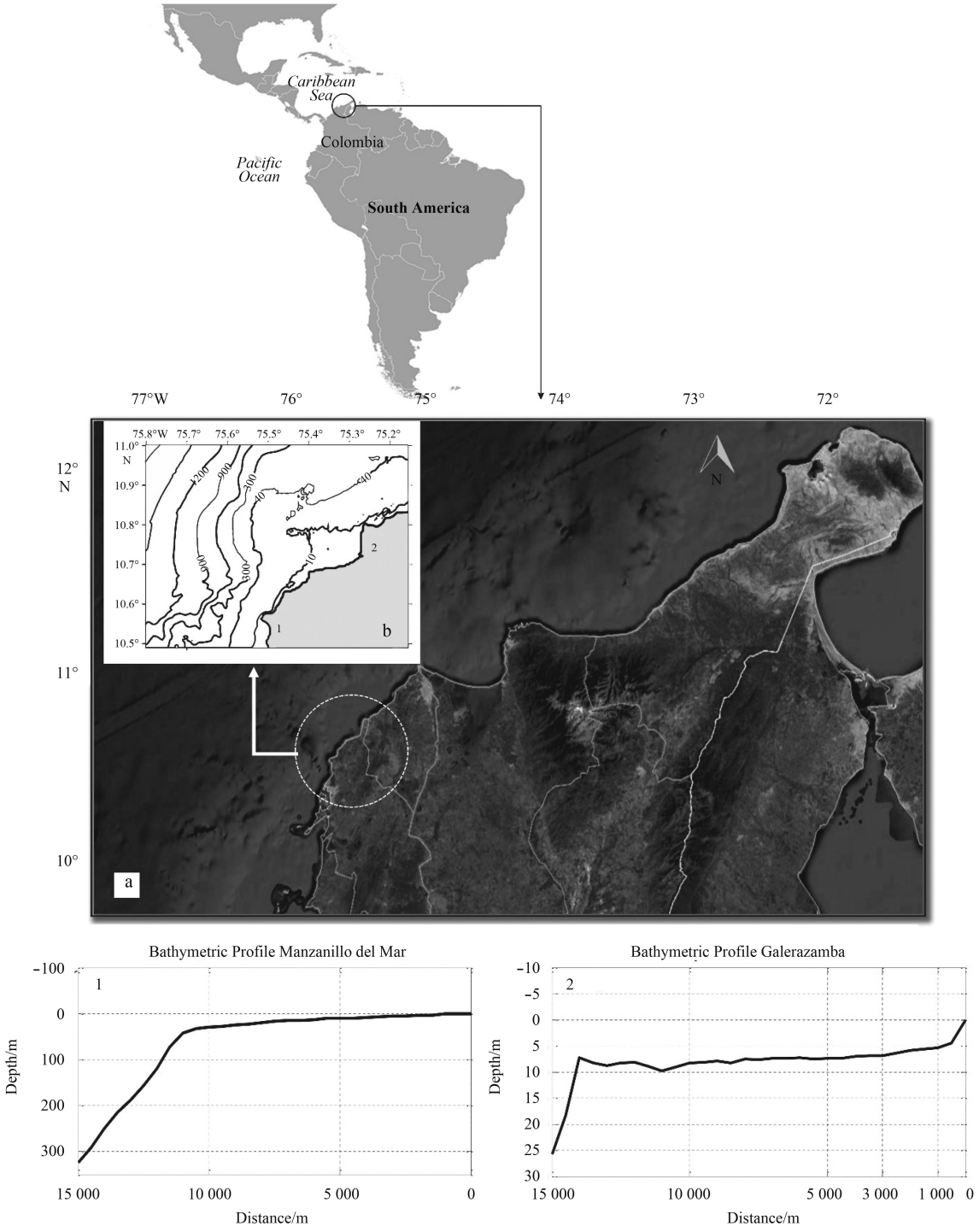

Fig. 1. Study area. a. Colombian Caribbean coast and b. Bathymetry study area (1. Manzanillo del Mar; 2. Galerazamba).

$$W_n(s) = \sum_{n'}^{N-1} x_{n'} \psi^* \left[\frac{(n'-n)\,\delta t}{s} \right], \tag{1}$$

where * indicates the complex xconjugate, ψ represents to the mother function (i.e., Morlet, Mexican Hat, Doubechies) and δt represents the temporal resolution. We used a Morlet wavelet, because of its good performance when working with wave time series (e.g., Ma et al., 2010, 2011).

The Normalize Morlet wavelet is defined as

$$\psi_o(\eta) = \pi^{-\frac{1}{4}} e^{i\omega_o \eta} e^{-\eta^2/2}, \tag{2}$$

where the subscript o indicates that the ψ must be normalized, ω_o is the non-dimensional frequency, and η is a dimensionless time parameter.

Through this process, it is possible to obtain information about a non-stationary time series for frequency, time and energy dimensions (Różyński, 2007), in order to determine which frequencies gain energy, as the wave approaches the coast.

2.3 *Signal pre-processing*

We subtracted the mean sea-level and trend from each data obtained by the sensors. Then, in order to apply the spectral

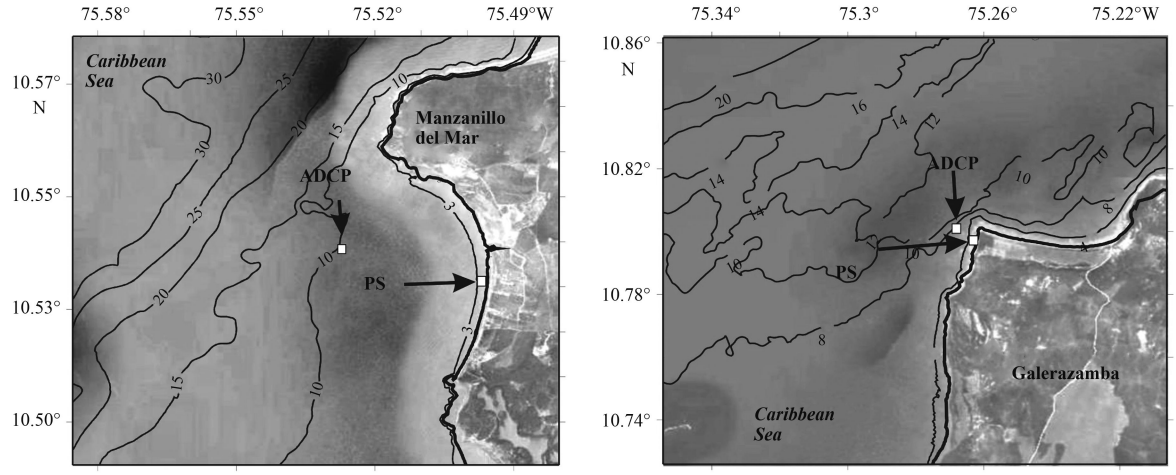

Fig. 2. Array equipment A. Manzanillo del Mar B. Galerazamba. White box indicates the ADCP and the pressure sensor (PS) position.

treatment, we transformed pressure time series to surface elevation time series by a transfer function based on linear theory, the same used in Lara et al. (2004). Figure 3 shows the time series measured by ADCP before and after these techniques; it also shows the long save component within the pressure time series.

After noting infragravity contribution in each beach during both seasons, we applied a finite impulse response band pass filter (FIR) with 1 121 coefficients (e.g., Soe et al., 2008), to obtain the infragravity signal in each season, the cut off frequencies chosen for the infragravity band were 0.003 Hz<f<0.05 Hz. The lower limit was set according to Brinkkemper et al. (2013) to avoid the contribution of larger waves than infragravity waves.

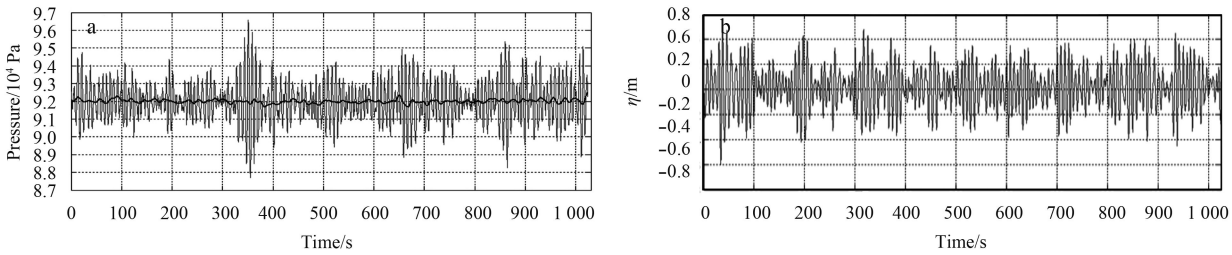

Fig. 3. Pressure time series obtained by the ADCP (thin line) and long wave component (dark line) (a), and surface elevation time series measured by the ADCP (b).

3 Results and discussion

Figure 4 shows the significant wave height time series (H_s) measured by the ADCP for both beaches during the two periods. It is evident that Galerazamba presented more energetic waves during the dry period, consistent with the fact that it is more exposed to waves than Manzanillo del Mar. We observed that Galerazamba presented significant variation of H_s during the dry season, due to the high pressure system of the Azores. This brought as a consequence that in the April's last week the winds on the Caribbean coast increased and therefore the incident waves (Duran et al., 2012). However, during the rainy period, the wave energy of Galerazamba was slightly higher than Manzanillo del Mar (Fig. 4).

For average condition, the spectral analysis applied to the surface elevation time series (chosen from an specific date with the same H_s of the average condition) show that gravity waves in Galerazamba are more energetic than Manzanillo del Mar in the two periods (Figs 5 and 6), and we could also observed that there is energy contribution in the low frequency band. Upon finding the energy contribution in low frequency bands, we applied the FIR filter with 1 121 coefficients to each surface elevation time series.

Figure 7 shows infragravity signals of Manzanillo del Mar and Galerazamba received by the ADCP during the dry period and Fig. 8 shows the infragravity signal for both beaches during the rainy period. From these figures, it is possible to observe that the infragravity signal is stronger in Galerazamba than Manzanillo del Mar. Specially, the height variation in the surface elevation does not exceed 3 cm during the dry period and 1.5 cm during the rainy period, the small amplitude suggest that this wave is still forced by a wave group. In order to verify if the infragravity wave is still forced by the wave group, the comparison between this wave and the envelopment of the short waves was made.

In Figs 9a–d, the cross correlation analysis shows a negative correlation between the envelopment of the short waves and the long waves at the travel time zero, for the beaches of Galerazamba and Manzanillo del Mar during the two periods, suggesting that the infragravity waves are still forced by the wave group at the ADCP. However, to confirm that the infragravity energy is due to the release of bound long waves, the cross correlation analysis between the envelopment of the short waves at the ADCP and the long waves at the pressure sensor was applied for the two beaches and both periods (dry period and wet period). In Figs 9e–h the results of the cross-correlation analysis are shown. From these graphs it is possible to notice that in the time required to travel from the ADCP to the pressure sensor, the cross correlation for the two beaches during both periods was negative which confirms that the IG energy is generated by the release of

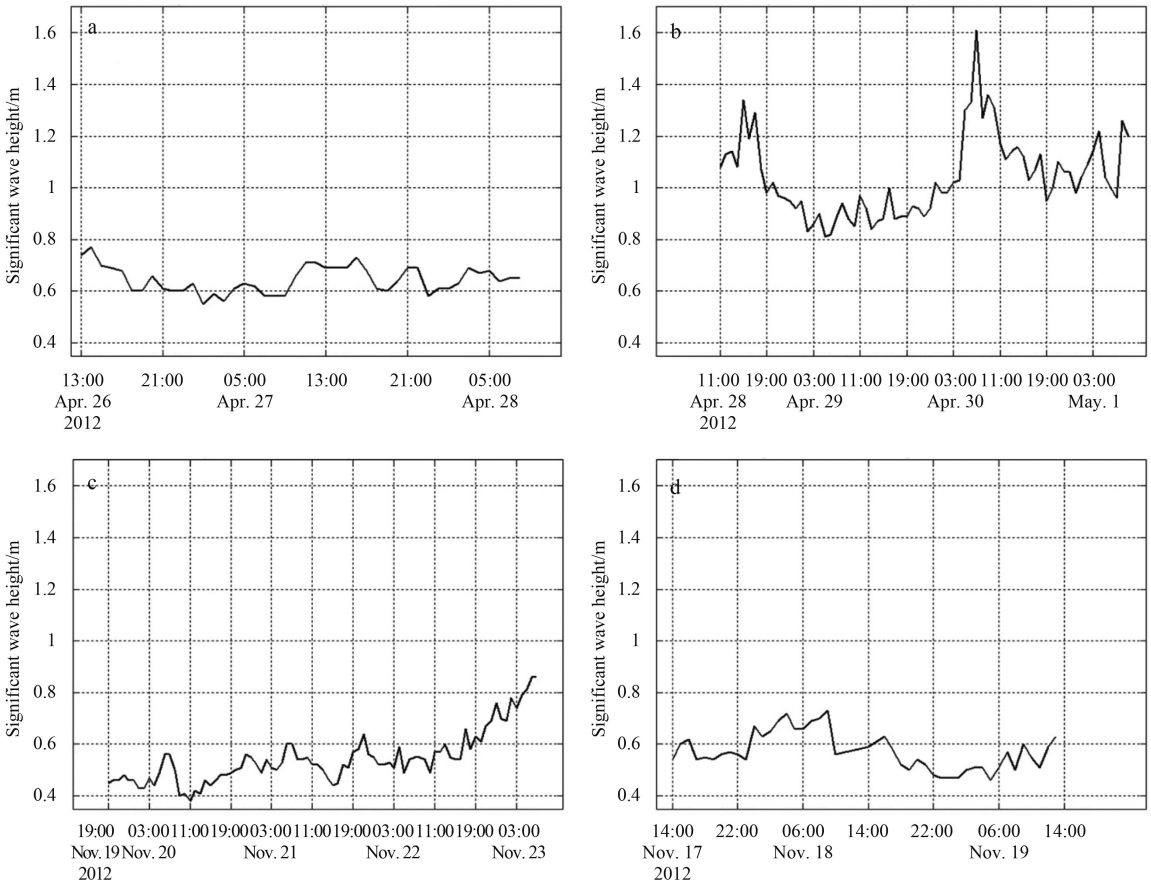

Fig. 4. H_s time series during the dry and rainy periods. a. H_s time series for Manzanillo del Mar during the dry period, b. H_s time series for Galerazamba during the dry period, c. H_s time series for Manzanillo del Mar during the rainy period, and d. H_s time series for Galerazamba during the rainy period.

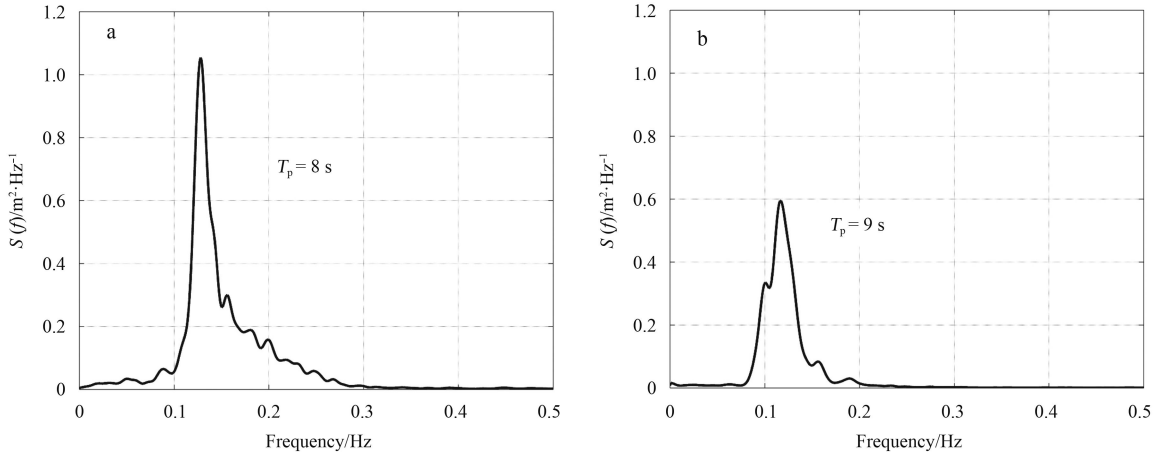

Fig. 5. Welch spectra for the surface elevation time series of Galerazamba (a) and Manzanillo del Mar (b) during the dry period.

bound long waves.

We applied the above procedure to the time series measured by the pressure sensor. Spectral analysis (Fig. 10) shows that wave energy measured by the pressure sensor during the dry period is lower than the measured by the ADCP (Figs 5 and 6), probably due to wave energy loss resulting from phenomena such as wave breaking and bottom friction; a similar situation occurs with the spectra measured by the same sensor during the rainy period. In addition to this, we could observe swell waves due to decreased local wind waves producing sea waves in the spectra of measurements carried out during this period.

Once we have identified the infragravity component in the spectra of the data measured by the pressure sensor, we filtered it and obtained higher values of surface elevation (Fig. 11) than those measured by the ADCP (Figs 7 and 8). This result is consistent with the fact that the maximum infragravity energy is usually

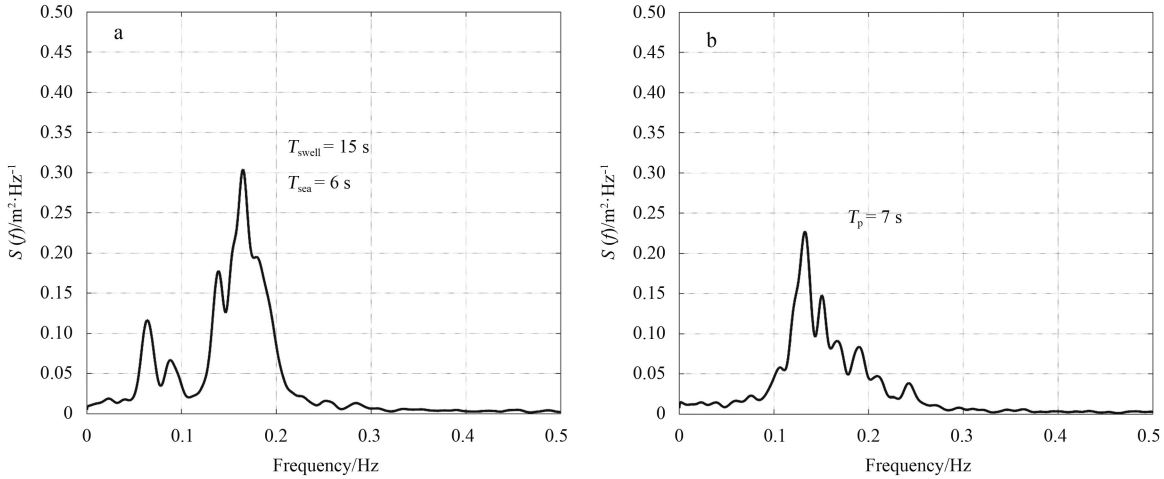

Fig. 6. Fourier spectra for the surface elevation time series of Galerazamba (a) and Manzanillo del Mar (b) during the rainy period (RP).

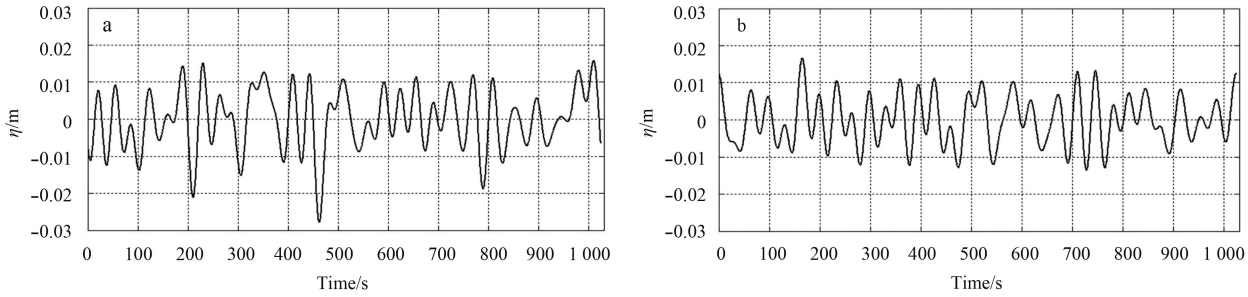

Fig. 7. Infragravity signal measured by the ADCP in Galerazamba (a) and infragravity signal measured by the ADCP in Manzanillo del Mar (b) during the dry period.

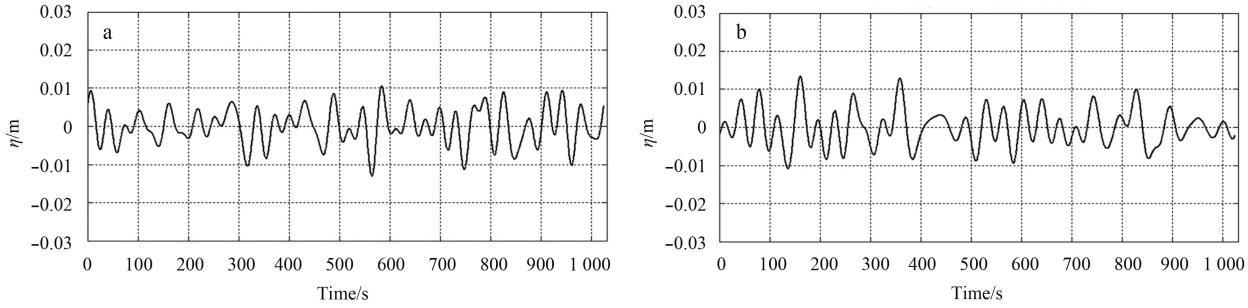

Fig. 8. Infragravity signal measured by the ADCP in Galerazamba (a) and infragravity signal measured by the ADCP in Manzanillo del Mar (b) during the rainy period.

found in the surf and swash zone (Oltman-Shay and Guza, 1987).

Figure 11 shows that maximum amplitude of the infragravity signal is higher during the dry period than the rainy period where maximum amplitudes recorded values do not exceed 4 cm. This agrees with Ruessink (1998a), who states that the higher the energy of the incident wave, the higher the energy of the infragravity component.

3.1 *Extreme condition*

During these campaigns, we could identify the most energetic sea states for Manzanillo and Galerazamba beaches. The most energetic wave event in Galerazamba presented a significant wave height of 1.61 m, while for Manzanillo del Mar the highest significant wave height was 0.86 m. We also applied spectral analysis to the time series measured by ADCP and the pressure sensor during these extreme conditions (Figs 12 and 13). These spectra show how the energy of the high frequencies decreases due to the wave breaking and bottom friction as the waves approaches to the shore, while the low-frequencies energy (infragravity waves) increases, these findings shows that in the beaches of Galerazamba and Manzanillo del Mar, the role of infragravity waves is very important (in terms of energy) because the energy associated to the infragravity waves do not dissipate as the waves approach to the coast, while the energy associated to the gravity waves dissipate as the waves approach to the coast.

By filtering the infragravity signal for Galerazamba (Fig. 14) we could observe that the maximum height measured by the ADCP was 8 cm. When the infragravity waves is measured by the

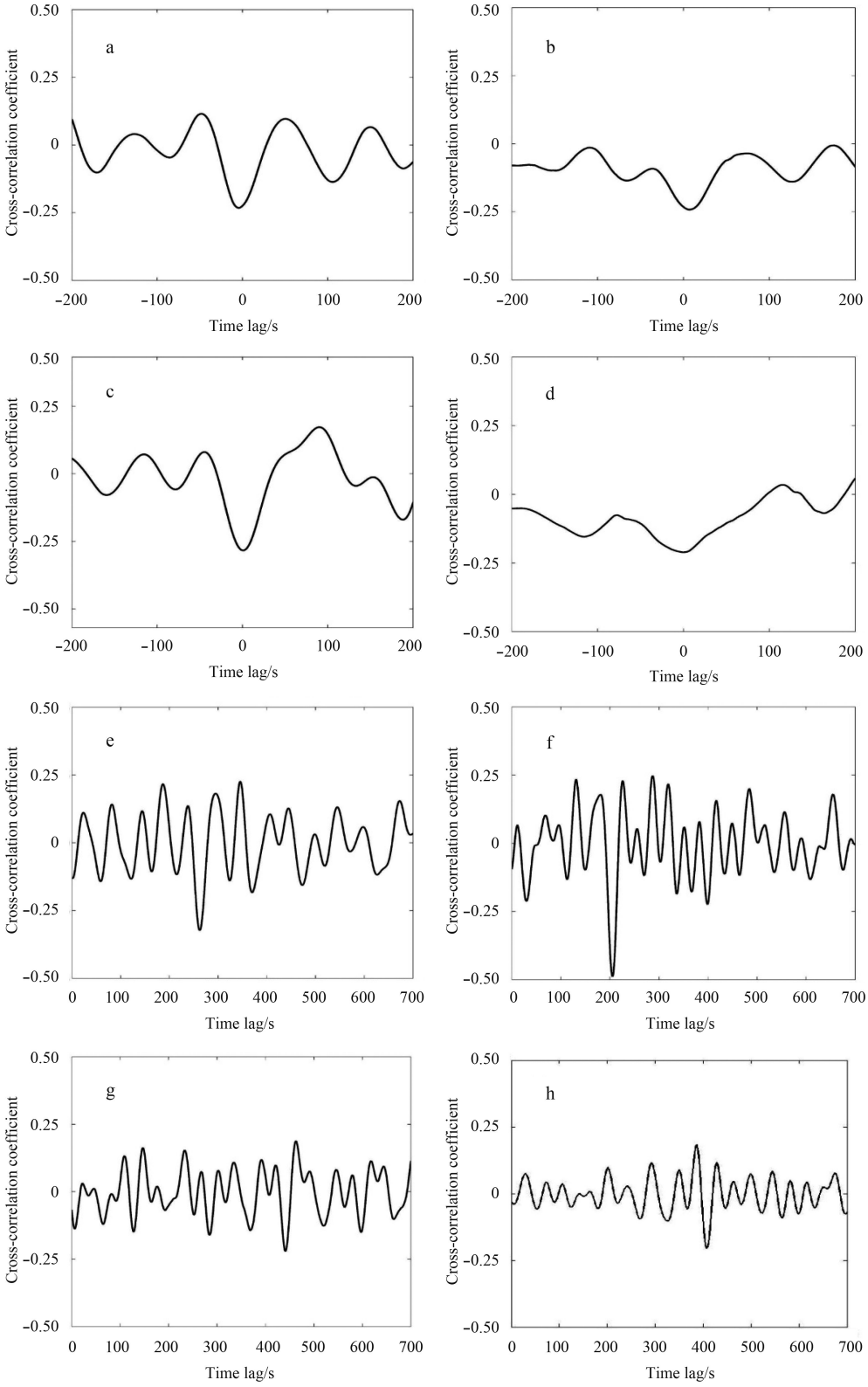

Fig. 9. Cross correlation between the short wave envelopment and the infragravity wave at ADCP. a. Galerazamba during dry period, b. Galerazamba during rainy period, c. Manzanillo del Mar during dry period, and d. Manzanillo del Mar during rainy period. Cross correlation analysis between the envelopment of the short waves at the ADCP and the long waves in the pressure sensor. e. Galerazamba during dry period, f. Galerazamba during rainy period, g. Manzanillo del Mar during dry period, and h. Manzanillo del Mar during rainy period.

pressure sensor the maximum height found was 18 cm. This corresponds to an increase of 125% compared to the ADCP measurement, it is important to note that this increase is given for a significant wave height of 1.6 m (the maximum value recorded

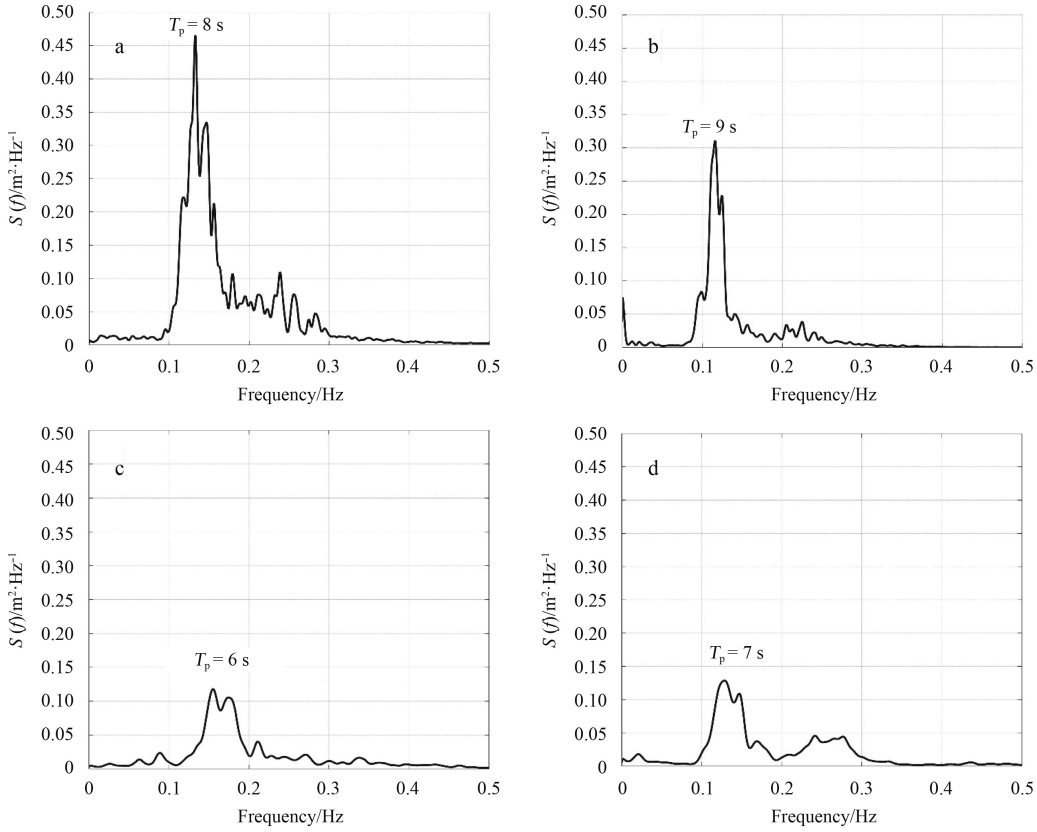

Fig. 10. Fourier spectra measured by the pressure sensor during the dry period: a. Galerazamba and b. Manzanillo del Mar, and rainy period: c. Galerazamba and d. Manzanillo del Mar.

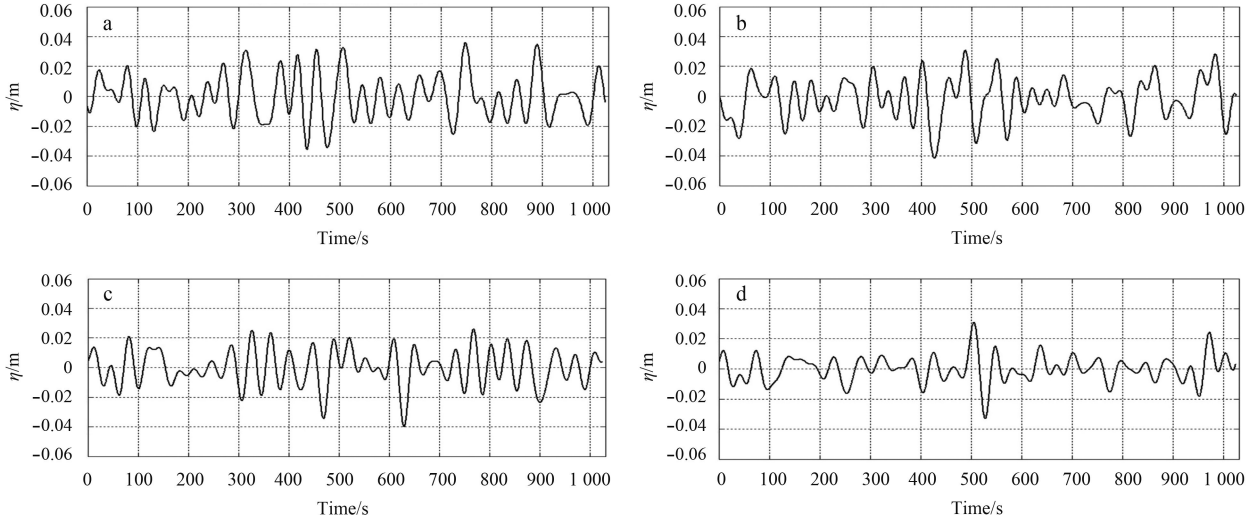

Fig. 11. Infragravity signal measured by the pressure sensor during the dry period: a. Galerazamba and b. Manzanillo del Mar, and rainy period: c. Galerazamba, and d. Manzanillo del Mar.

during the campaign). However, the increase may be much higher when appearing more energetic wave conditions, highlighting the importance of these oscillations in the coastal flooding phenomena. On the other side, the maximum height measured by the ADCP in Manzanillo del Mar was 5 cm. When the infragravity waves is measured by the pressure sensor the maximum height found was 8 cm. This corresponds to an increase of 60% compared to the ADCP measurement (Fig. 15).

3.2 *Wavelet analysis*

Finally, we calculated the wavelet spectrum to determine the information of the magnitude, frequency and temporal occurrence of long-wave energy packages in surface elevation time series measured during the extreme condition. The surface elevation time series of the sea-swell band for the beaches of Galerazamba and Manzanillo del Mar are shown (Figs 16a and 17a) with its wavelet spectrum (Figs 16b, 16c, 17b, and 17c) as well as, the surface elevation time series of the infragravity band

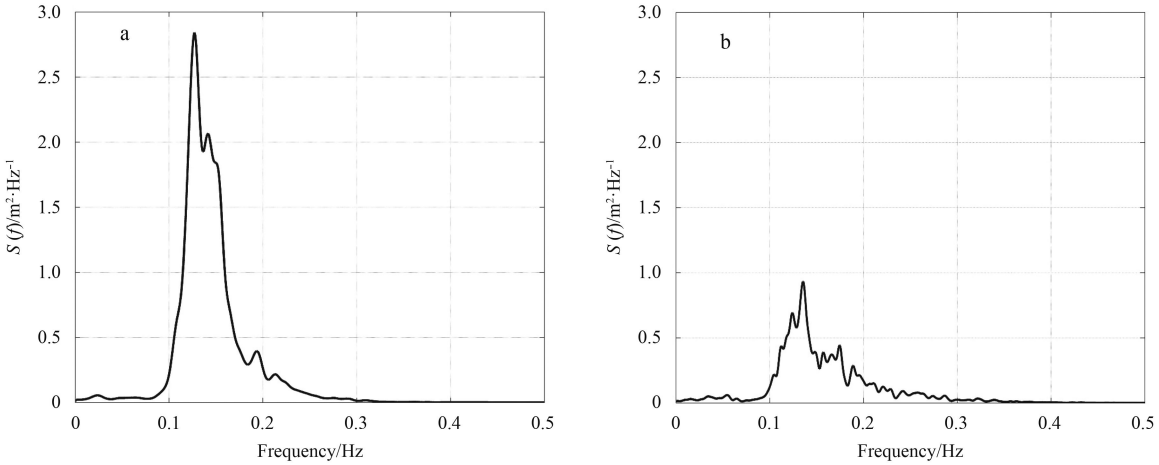

Fig. 12. Welch spectrum for Galerazamba during an extreme wave condition. a. ADCP outside the surf zone and b. pressure sensor inside the surf zone.

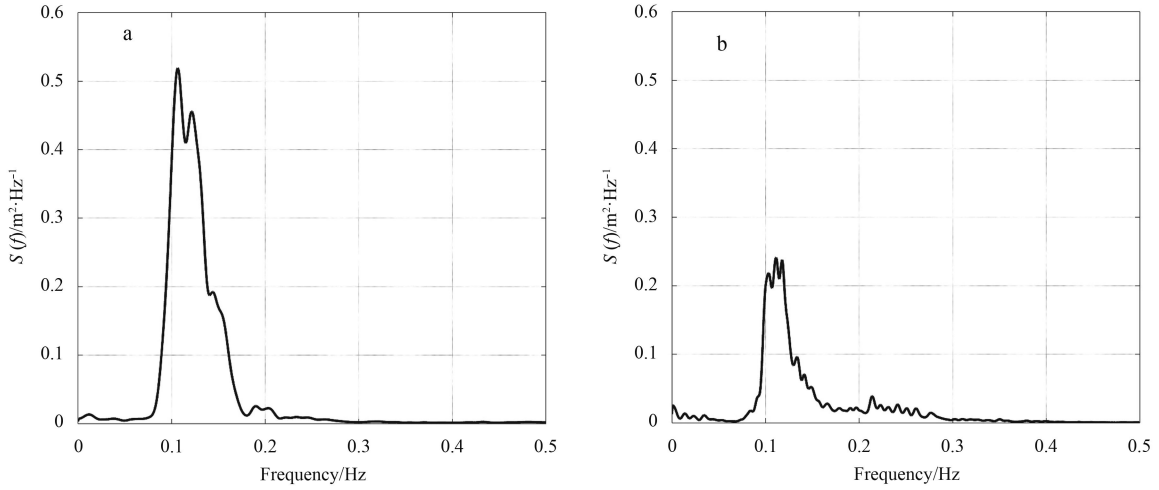

Fig. 13. Welch spectrum for Manzanillo del mar during an extreme wave condition. a. ADCP outside the surf zone and b. pressure sensor inside the surf zone.

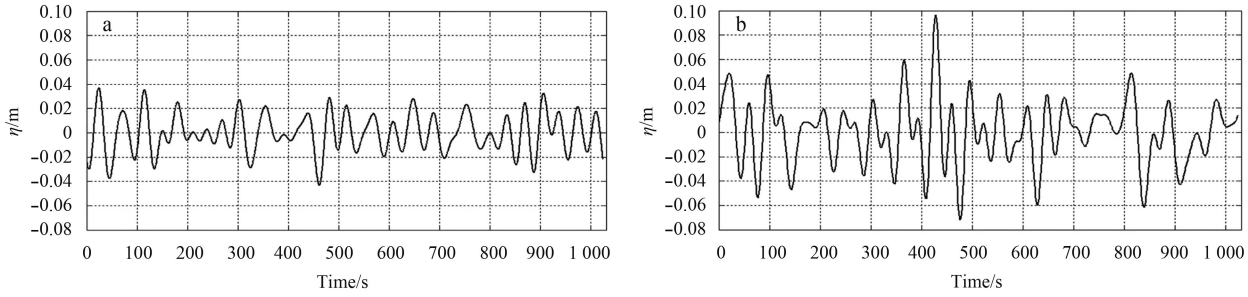

Fig. 14. Infragravity signal in Galerazamba during the more energetic wave event as measured by ADCP (a) and pressure sensor (b).

and its wavelets spectra for the ADCP (Figs 16d, 16e, 16f, 17d, 17e, and 17f).

For Galerazamba the wavelet analysis shows that energy is concentrated around the peak period of 8 s throughout the burst duration. This result is consistent with the spectral analysis (PSD) of the same series (Fig. 12a) which evidences the frequency with the maximum energy is 0.125 Hz (T=8 s). However, at low frequencies it is not possible to determine which ones have higher energies in the infragravity band. Therefore, by applying the wavelet analysis to the infragravity band, it is possible to identify that the highest energy contribution takes place at a frequency of about 0.020 Hz (T=48 s) (Fig. 16f).

Figures 18 and 19 show the results for the pressure sensor for both beaches. It is evident that the wave in sea-swell band keeps its maximum energy in a period of 8 s (Figs 18c and 19c). However, when comparing the energy values of both sensors we

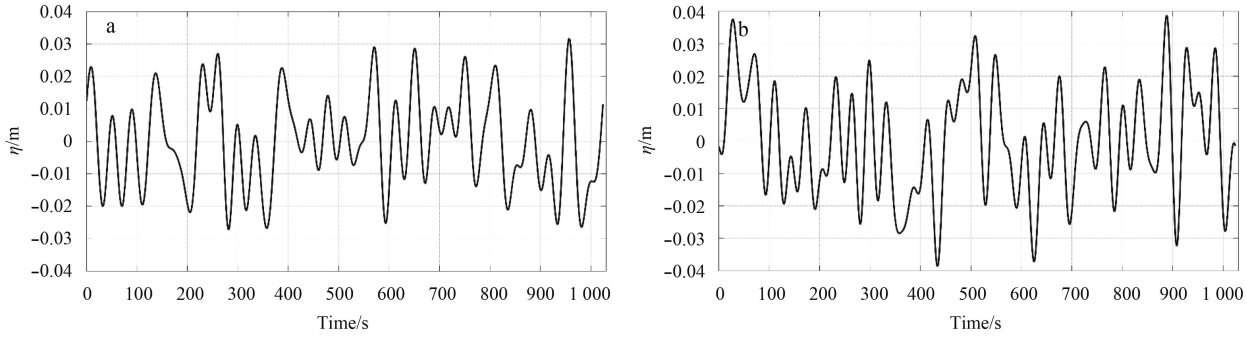

Fig. 15. Infragravity signal in Manzanillo del Mar during the more energetic wave event as measured by ADCP (a) and pressure sensor (b).

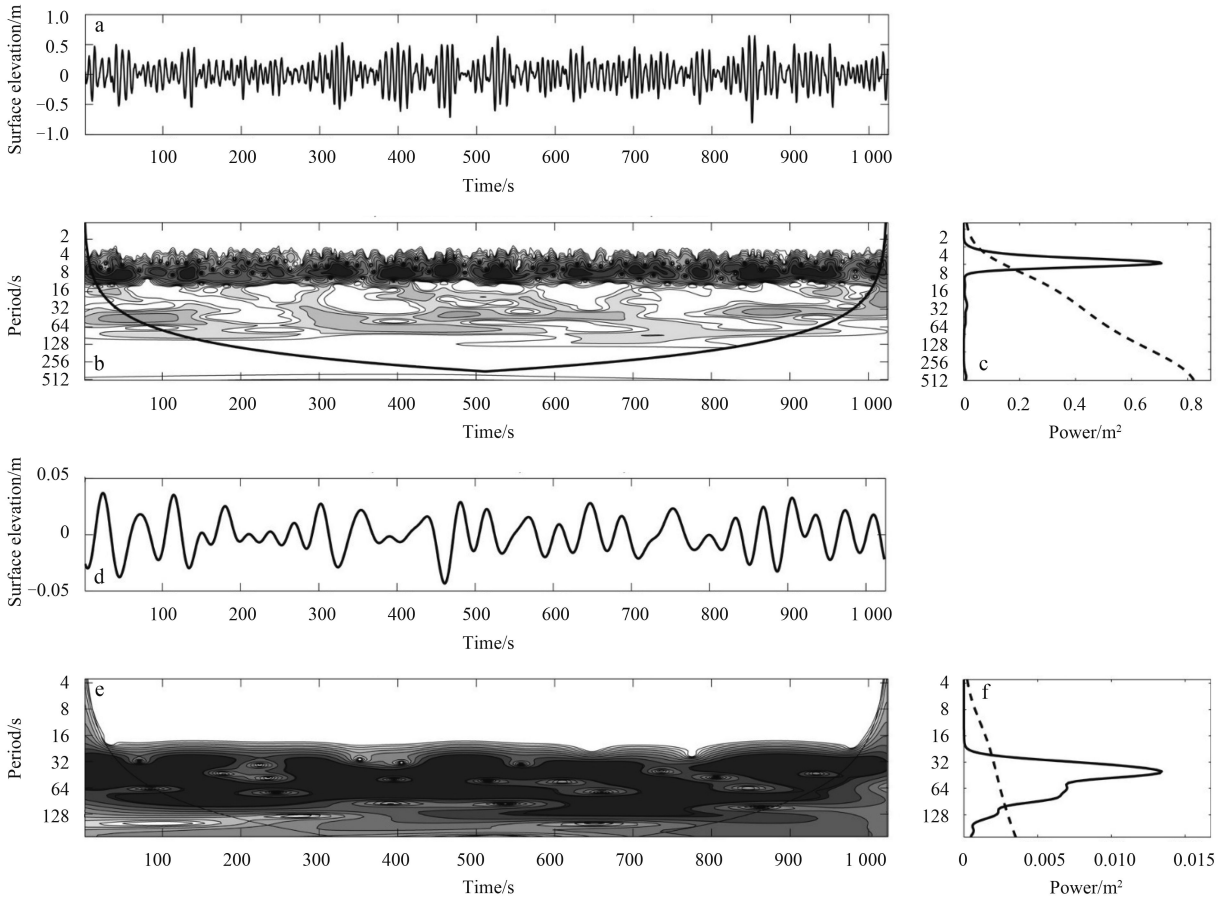

Fig. 16. Surface elevation time series for sea-swell and infragravity band measured with ADCP in Galerazamba. a. Surface elevation for sea-swell band, b. surface elevation wavelet power spectrum for sea-swell band, c. global wavelet spectrum for sea-swell band, d. surface elevation time series for infragravity, e. surface elevation wavelet power spectrum for infragravity band, and f. global wavelet spectrum for infragravity band.

found that the energy value in the pressure sensor is lower for the gravitational band. This result confirms our findings through Welch spectra regarding the surface elevation signals measured by the ADCP and the pressure sensor during the highest energy event. On the other hand, Figs 18f and 19f show frequencies that appear in the infragravity band with higher energy. When comparing Figs 16f to 18f we can observe that the energy of the highest frequencies lose energy while the lower frequencies gain energy as waves approach the shore, since the period 48 s component loses energy, and the 64 s period component gain energy. For Manzanillo del Mar, we observe a similar behavior, because Figs 17f and 19f show an energy loss from highest frequencies and an energy gain for the lower frequencies as waves approach the shore (the period of 32 s losses energy, while the 64 s period component gains energy).

These results agree with those found by de Bakker et al. (2014) where it is shown that in a dissipative beach the energy of the high frequencies decrease, while energy of the low frequencies increase. On the other hand, it is also possible to observe that the infragravity frequencies presented near to the shore for

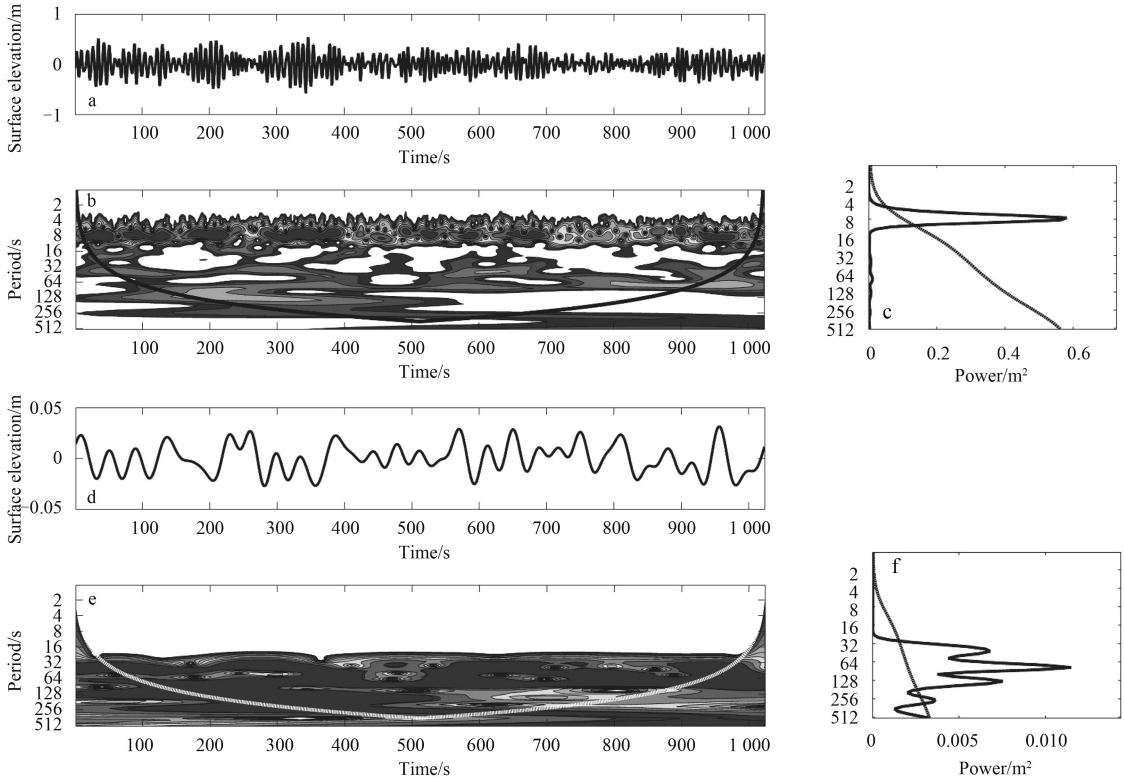

Fig. 17. Surface elevation time series for sea-swell and infragravity band measured with ADCP in Manzanillo del Mar. a. Surface elevation for sea-swell band, b. surface elevation wavelet power spectrum for sea-swell band, c. global wavelet spectrum for sea-swell band, d. surface elevation time serie for infragravity, e. surface elevation wavelet power spectrum for infragravity band, and f. global Wavelet Spectrum for infragravity band.

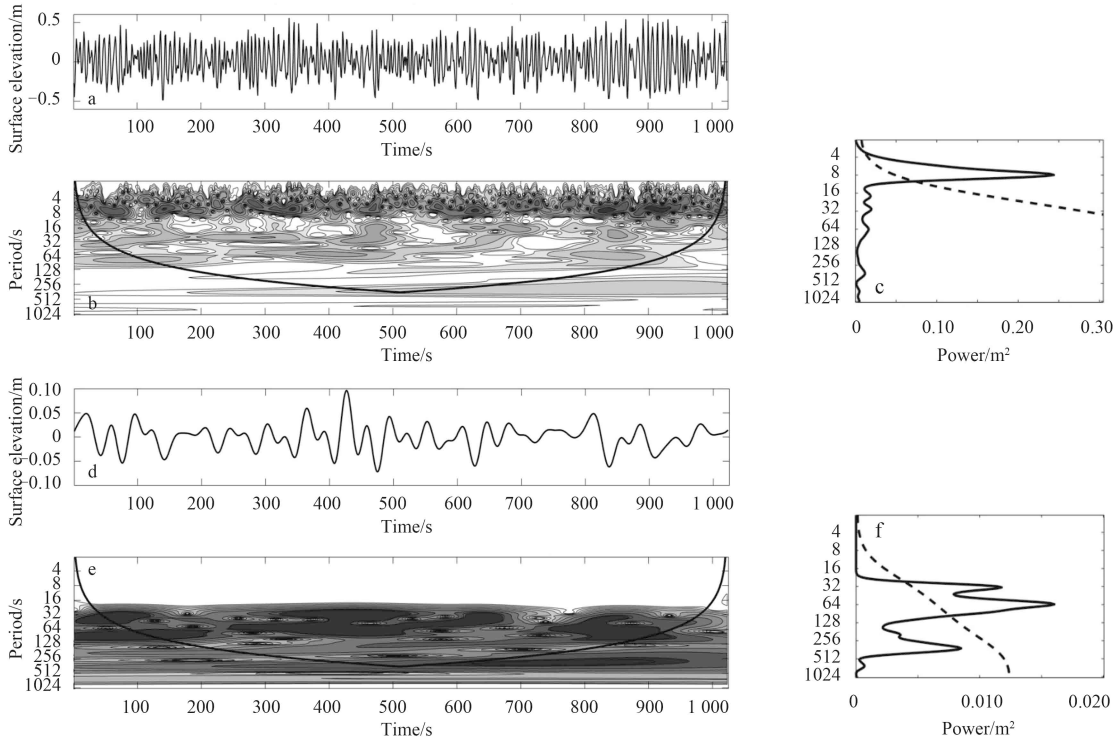

Fig. 18. Surfac e elevation time serie for sea-swell and infragravity band measured with pressure sensor in Galerazamba. a. Surface elevation for sea-swell band, b. surface elevation wavelet power spectrum for sea-swellband, c. global wavelet spectrum for sea-swell band, d.surface elevation time serie for infragravity, e. surface elevation wavelet power spectrum for infragravity band, and f. global wavelet spectrum for infragravity band.

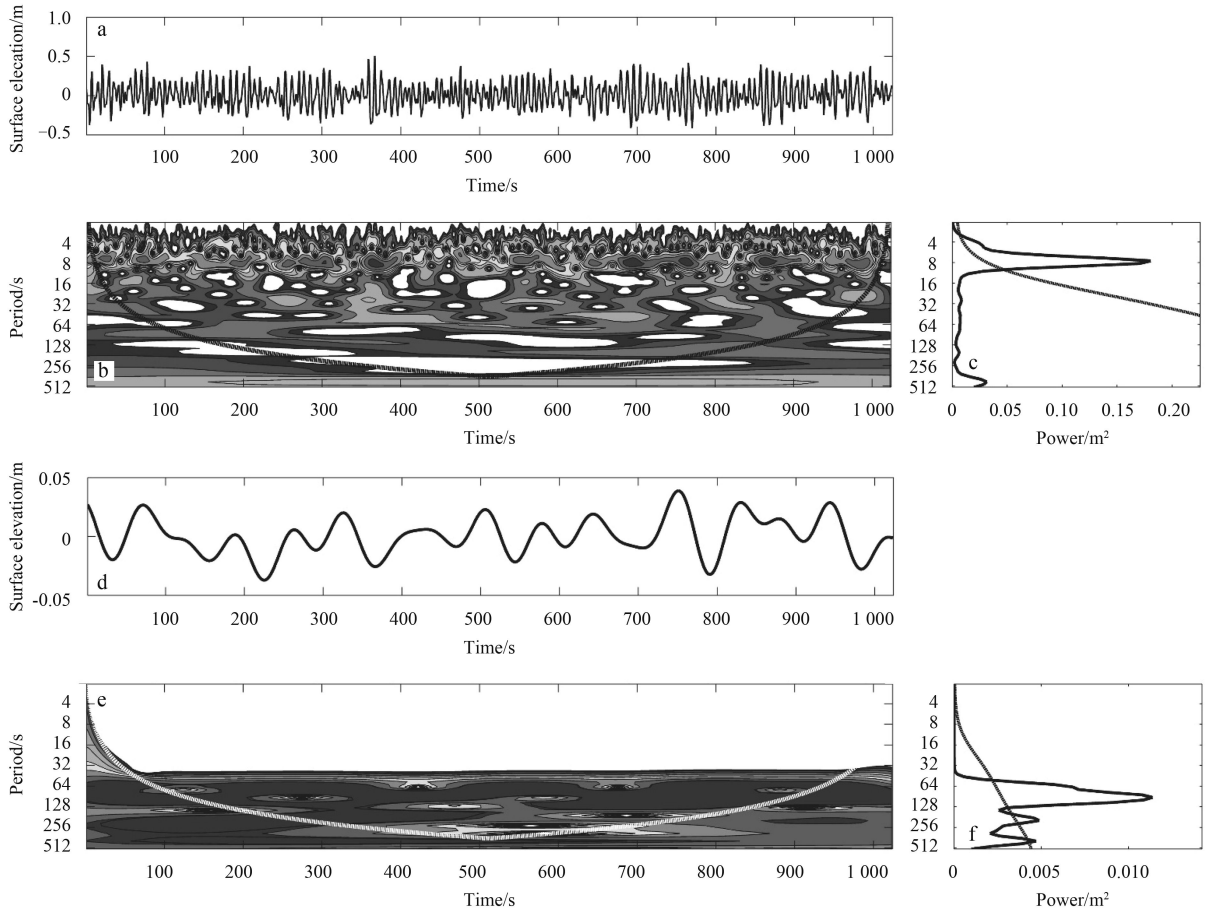

Fig. 19. Surface elevation time series for sea-swell and infragravity band measured with pressure sensor in Manzanillo del mar. a. Surface elevation for sea-swell band, b. surface elevation wavelet power spectrum for sea-swell band, c. global wavelet spectrum for sea-swell band, d. surface elevation time series for infragravity, e. surface elevation wavelet power spectrum for infragravity band, and f. global Wavelet Spectrum for infragravity band.

Galerazamba range from 0.020 8 Hz (T=48 s) to 0.015 6 Hz (T=64 s), and for Manzanillo del Mar range from 0.031 2 (T=32 s) to 0.015 6 Hz (T=64 s). These values are lower than the values found by de Bakker et al. (2014), suggesting that the infragravity energy that is present in these beaches does not dissipate as they reach the coast. While, the gravity (sea-swell) energy will dissipate due the wave breaking and bottom friction.

It is important to note that although Fig. 18f shows an energy contribution in the 500 s period component, in Fig. 18e this component is below the curve of statistical significance and it should not be considered.

4 Conclusions

We have carried out an experimental infragravity wave analysis for two case studies of dissipative beaches (Galerazamba and Manzanillo del Mar). Based on the spectral analysis of surface elevation time series, we found that the frequencies' energy in the sea-swell band decreases due to wave breaking and bottom friction as the wave approaches the coast, while the energy of some frequencies in the infragravity band increases. However, it is not possible to identify which of the components within the infragravity band gain energy as the wave approaches the coast from this analysis because the energy of the infragravity frequencies does not follow a known pattern.

Through the wavelet analysis, we found that the energy from the sea-swell decrease, while the energy of the infragravity band increases as the wave approaches the coast (as shown in the above discussion from Fourier analysis). However, we could determine within the infragravity band the frequencies that have higher energy, thus determining that the energy within the infragravity band is gained by the lowest frequencies as the wave approaches the shore. It was also possible to find that the frequencies that gain energy while the waves reach the coast are lower than 0.016 7 Hz, hence we can conclude that the energy associated with these frequencies does not dissipate as waves approach the coast.

By filter the infragravity wave from the maximum wave event recorded during the field campaign in Galerazamba and Manzanillo del Mar, we can hint the importance of the contribution of this signal in coastal flooding processes, since it was 18 cm (Galerazamba) and 8 cm (Manzanillo del Mar) high when measured near the coast, i.e., 125% and 60% higher than the average condition for Galerazamba and Manzanillo del Mar. From the wavelet analysis, we establish that these waves play an important role on morphological changes, because we were able to determine the frequencies of these waves that gain energy as they approach the coast and by comparing these frequencies with the frequencies found from de Bakker et al. (2014) for a dissipative beach establish that the energy of infragravity frequencies presented in both beaches do not dissipate as they approach to

the coast. We therefore believe the infragravity waves should be taken into account in the processes of coastal flooding and also on morphological changes on dissipative beaches.

Acknowledgements

The authors thank to the I+D+I Department of the Universidad del Norte, and the reviewers for the suggestions and constructive comments on an earlier draft of this manuscript.

References

Aagaard T, Bryan K R. 2003. Observations of infragravity wave frequency selection. Continental Shelf Research, 23(10): 1019–1034

Battjes J A, Bakkenes H J, Janssen T T, et al. 2004. Shoaling of subharmonic gravity waves. Journal of Geophysical Research: Oceans (1978–2012), 109(C2): C02009

de Bakker A T M, Tissier M F S, Ruessink B G. 2014. Shoreline dissipation of infragravity waves. Continental Shelf Research, 72: 73–82

Dong Guohai, Ma Yuxiang, Ma Xiaozhou. 2008. Cross-shore variations of wave groupiness by wavelet transform. Ocean Engineering, 35(7): 676–684

Dong Guohai, Ma Xiaozhou, Perlin M, et al. 2009a. Experimental study of long wave generation on sloping bottoms. Coastal Engineering, 56(1): 82–89

Dong Guohai, Ma Xiaozhou, Teng Bin. 2009b. Numerical modeling of surf beat generated by moving breakpoint. Science in China Series E: Technological Sciences, 52(2): 392–399

Duran J C, Acosta J, Murillo N, et al. 2012. Seguimiento de las condiciones meteorológicas y oceanográficas en el caribe colombiano 2012. Technical Report No 160. Cartagena, Colombia: Dirección General Marítima, Written in Spanish

Eckart C. 1952. The propagation of gravity waves from deep to shallow water. In: Gravity Waves. National Bureau of Standards Circular 521. Washington, D C: U S. Government Printing Office, 165

Elgar S, Guza R T. 1985. Observations of bispectra of shoaling surface gravity waves. Journal of Fluid Mechanics, 161: 425–448

Elgar S, Herbers T H C, Okihiro M, et al. 1992. Observations of infragravity waves. Journal of Geophysical Research: Oceans (1978–2012), 97(C10): 15573–15577, doi: 10.1029/92JC01316

Guza R T, Thornton E B. 1982. Swash oscillations on a natural beach. Journal of Geophysical Research: Oceans (1978–2012), 87(C1): 483–491

Henderson S M, Bowen A J. 2002. Observations of surf beat forcing and dissipation. J Geophys Res, 107(C11): 14–1–14–10

Henderson S M, Guza R T, Elgar S, et al. 2006. Nonlinear generation and loss of infragravity wave energy. Journal of Geophysical Research: Oceans (1978–2012), 111(C12): C12007

Herbers T H C, Elgar S, Guza R T. 1994. Infragravity-frequency (0.005–0.05 Hz) motions on the shelf. Part I: forced waves. Journal of Physical Oceanography, 24(5): 917–927

Holman R A, Bowen A J. 1982. Bars, bumps, and holes: models for the generation of complex beach topography. Journal of Geophysical Research: Oceans (1978–2012), 87(C1): 457–468

Holman R A, Sallenger A H Jr. 1985. Setup and swash on a natural beach. Journal of Geophysical Research: Oceans (1978–2012), 90(C1): 945–953

Huang M C. 2004. Wave parameters and functions in wavelet analysis. Ocean Engineering, 31(1): 111–125

Lara J L, Martin F L, Losada I J, et al. 2004. Experimental analysis of long waves at harbour entrances. In: Proceedings of the 29th International Conference. Lisbon, Portugal: National Civil Engineering Laboratory

Lin Y H, Hwung H H. 2012. Infra-gravity wave generation by the shoaling wave groups over beaches. China Ocean Engineering, 26(1): 1–18

Liu P C. 1994. Wavelet spectrum analysis and ocean wind waves. Wavelet Analysis and Its Applications, 4: 151–166

Longuet-Higgins M S, Stewart R W. 1962. Radiation stress and mass transport in gravity waves, with application to 'surf beats'. Journal of Fluid Mechanics, 13(4): 481–504

Ma Yuxiang, Dong Guohai, Ma Xiaozhou, et al. 2010. A new method for separation of 2d incident and reflected waves by the Morlet wavelet transform. Coastal Engineering, 57(6): 597–603

Ma Yuxiang, Dong Guohai, Ma Xiaozhou. 2011. Separation of obliquely incident and reflected irregular waves by the Morlet wavelet transform. Coastal Engineering, 58(8): 761–766

Massel S R. 2001. Wavelet analysis for processing of ocean surface wave records. Ocean Engineering, 28(8): 957–987

Morlet J, Arens G, Fourgeau E, et al. 1982. Wave propagation and sampling theory-Part I: complex signal and scattering in multilayered media. Geophysics, 47(2): 203–221

Munk W H. 1949. Surf beats. EOS Transaction American Geophysical Union, 30(6): 849–854

Oltman-Shay J, Guza R T. 1987. Infragravity edge wave observations on two california beaches. Journal of Physical Oceanography, 17(5): 644–663

Ortiz-Royero J C, Otero L J, Restrepo J C, et al. 2013. Cold fronts in the colombian Caribbean sea and their relationship to extreme wave events. Natural Hazards and Earth System Science, 13(11): 2797–2804

Rangel-Buitrago N G, Anfuso G, Williams A T. 2015. Coastal erosion along the Caribbean coast of Colombia: magnitudes, causes and management. Ocean &Coastal Management, 114: 129–144

Restrepo J C, Otero L, Casas A C, et al. 2012. Shoreline changes between 1954 and 2007 in the marine protected area of the Rosario island archipelago (Caribbean of Colombia). Ocean &Coastal Management, 69: 133–142

Różyński G. 2007. Infragravity waves at a dissipative coast; evidence upon multi-resolution analysis. Coastal Engineering, 54(3): 217–232

Ruessink B G. 1998a. The temporal and spatial variability of infragravity energy in a barred nearshore zone. Continental Shelf Research, 18(6): 585–605

Ruessink B G. 1998b. Bound and free infragravity waves in the nearshore zone under breaking and nonbreaking conditions. Journal of Geophysical Research: Oceans (1978–2012), 103(C6): 12795–12805, doi: 10.1029/98JC00893

Soe N M, Jannat M R A, Asano T. 2008. Transformation of short wave groups and generation of infragravity waves on a bar-type beach. In: Proceedings of the 18th International Offshore and Polar Engineering Conference. Vancouver, BC, Canada: The International Society of Offshore and Polar Engineers

Symonds G, Huntley D A, Bowen A J. 1982. Two-dimensional surf beat: long wave generation by a time-varying breakpoint. Journal of Geophysical Research: Oceans (1978–2012), 87(C1): 492–498

Torrence C, Compo G P. 1998. A practical guide to wavelet analysis. Bulletin of the American Meteorological Society, 79(1): 61–78

Van Dongeren A, Battjes J, Janssen T, et al. 2007. Shoaling and shoreline dissipation of low-frequency waves. Journal of Geophysical Research: Oceans (1978–2012), 112(C2): C02011

Webb S C, Zhang X, Crawford W. 1991. Infragravity waves in the deep ocean. Journal of GeophysicalResearch: Oceans (1978–2012), 96(C2): 2723–2736

Wright L D, Nielsen P, Shi N C, et al. 1986. Morphodynamics of a bar-trough surf zone. Marine Geology, 70(3–4): 251–285

Wright L D, Short A D. 1984. Morphodynamic variability of surf zones and beaches: a synthesis. Mar Geol, 56(1–4): 93–118